Research Square

Preprints are preliminary reports that have not undergone peer review.
They should not be considered conclusive, used to inform clinical practice,
or referenced by the media as validated information.

Comparative mitogenomes of twelve Lasiocampidae species: genomic architecture, evolutionary dynamics, and phylogenomic implications

Ya-Lin Pu
Henan University
Yuan-Ke Li
Henan University
Jie Yang
Henan University
Kai Gao
gaokai@henu.edu.cn

Henan University

Research Article

Keywords: Comparative genomics, Lasiocampidae, lappet moths, Mitogenome, Phylogeny

Posted Date: October 14th, 2026

DOI: https://doi.org/10.21203/rs.3.rs-11091033/v1

License: This work is licensed under a Creative Commons Attribution 4.0 International License.
Read Full License

Additional Declarations: No competing interests reported.

Abstract

Background

Lasiocampidae is a diverse family of Lepidoptera that includes many significant defoliators of forest trees, yet its phylogenetic relationships remain poorly resolved. In this study, we sequenced and assembled the complete mitochondrial genomes of 12 lasiocampid species, 11 of which are reported here for the first time, to perform comparative genomic analyses and reconstruct a comprehensive phylogenetic framework for the family.

Results

Through next-generation sequencing, the 12 mitogenomes ranged from 15,387 bp to 15,938 bp in length and exhibited typical circular structures with high AT content. Gene order was conserved across all species except *Arguda vinata*, which possessed a unique *trnI–trnM–trnQ* arrangement. Evolutionary rates varied among PCGs: *nad6* and *atp8* evolved fastest, while *cox1* was most conserved. All PCGs were under strong purifying selection (ω << 1). Phylogenetic analyses recovered Lasiocampidae as a monophyletic group, with *Trabala* and *Crinocraspeda* forming the earliest diverging lineage. Among the highly supported sister-group relationships, *Dendrolimus* and *Pachypasoides* formed a clade with *Kunugia*.

Conclusions

This study substantially expands the mitogenomic resources for Lasiocampidae and provides a robust phylogenetic framework for the family. The findings clarify long-standing uncertainties in generic relationships and offer insights into mitochondrial evolution, including conserved genomic architecture and variable evolutionary rates among genes. These data will facilitate future systematic and evolutionary studies of Lasiocampidae.

Background

The family Lasiocampidae Harris, 1841 is a diverse group of moths within the order Lepidoptera, currently comprising approximately 2,000 described species across 229 genera, with the highest diversity concentrated in tropical and subtropical regions worldwide [1]. Adults of Lasiocampidae, commonly known as lappet moths, are characterized by their roof-like resting posture, in which the wavy-edged hindwings extend beyond the forewings, superficially resembling dead leaves [2]. These moths are predominantly nocturnal, with mouthparts that are greatly reduced or entirely absent, reflecting their limited adult feeding activity [3]. In contrast, their larvae, often called hairy caterpillars, are highly polyphagous and represent significant defoliators of forest trees, with host plants spanning multiple families, including Pinaceae, Fagaceae, Salicaceae, and Rosaceae [6]. During periodic outbreaks, the

gregarious feeding of these larvae can cause extensive defoliation, leading to substantial ecological disturbance within forest ecosystems and considerable economic losses in forestry production [3]. While recent morphological studies have provided detailed insights into the ultrastructure of larval mouthparts and adult antennal sensilla in several lasiocampids [5, 6], a comprehensive understanding of their population genetics, evolutionary history, and adaptive mechanisms remains limited. This is largely due to the scarcity of genomic resources, which are crucial for elucidating phylogenetic relationships and developing effective management strategies.

The mitochondrial genome (mitogenome) is a double-stranded circular DNA molecule, typically 14–20 kb in insects, characterized by maternal inheritance, rapid evolutionary rates, and conserved gene arrangement [7, 8]. It comprises two strands with asymmetric nucleotide composition: the J-strand (major coding strand) and the N-strand (minor coding strand) [9]. The insect mitogenome generally contains 37 genes: 13 protein-coding genes (PCGs) involved in oxidative phosphorylation, 22 transfer RNA (tRNA) genes, two ribosomal RNA genes (*rrnL* and *rrnS*), and one non-coding A + T-rich region that regulates replication and transcription [10]. Most tRNAs fold into a typical cloverleaf secondary structure, except for *trnS1*, which lacks the DHU arm [11]. The control region exhibits considerable length variation among species and individuals, contributing significantly to mitogenome size variation [12]. Among the 13 PCGs, start codons are predominantly ATN, with cox1 frequently utilizing the non-standard CGA in Lepidoptera [13]. The Ka/Ks ratios of PCGs are generally below 1, indicating purifying selection [14]. Owing to their compact size, rapid substitution rates, and conserved gene content, mitogenomes have been widely used for phylogenetic reconstruction, species delimitation, and population genetics in insects [15]. In Lepidoptera, mitogenomic data have proven effective in resolving evolutionary relationships across various taxonomic levels [16]. However, mitogenomic data for Lasiocampidae remain scarce, and the phylogenetic relationships and evolutionary history within this family are still largely unresolved.

Mitogenomes have been extensively applied to resolve phylogenetic relationships across Lepidoptera at multiple taxonomic levels [16]. Mitochondrial PCGs revealed that Hesperioidea nests within Papilionoidea, challenging traditional morphological classifications [17, 18]. At the family level, a recent mitogenomic study of *Trabala vishnou* recovered Lasiocampidae as sister to other bombycoid families, and phylogenetic trees based on 13 PCGs and two rRNAs further confirmed the monophyly of Lasiocampidae [19]. At the intraspecific level, mitochondrial markers have consistently demonstrated that *Bombyx mori* is more closely related to the Chinese wild silkworm than to the Japanese wild silkworm, supporting the Chinese origin of domesticated silkworms [20–22]. Similarly, mitochondrial DNA markers have revealed pronounced genetic differentiation among geographical populations of *Dendrolimus kikuchii*, closely associated with habitat fragmentation and limited dispersal ability [23]. Despite these advances, mitogenomic investigations of Lasiocampidae remain disproportionately scarce given the family's considerable diversity. Most existing studies have focused on a limited number of economically important species, while the phylogenetic relationships and evolutionary history across most genera and subfamilies within this group remain largely unexplored [13].

In this study, we sequenced and assembled the complete mitochondrial genomes of 12 lasiocampid species, 11 of which are reported here for the first time. We reconstructed the phylogenetic relationships of Lasiocampidae using these novel mitogenomes and outgroup data from other bombycoid taxa, based on concatenated sequences of 13 PCGs and two rRNAs. Our aims to: (1) characterize the structural features, nucleotide composition, codon usage, and evolutionary patterns of these novel mitogenomes; and (2) elucidate the phylogenetic relationships among the 12 focal species and clarify the intra-familial taxonomy of Lasiocampidae. This study will provide valuable genomic resources for future research on the systematics, evolution, and phylogeography of this economically important family.

Materials and Methods

Sample collection and DNA extraction

The samples used in this study were collected from various localities across China between July 2024 and August 2025 (Table 1). Specimens were preserved in 95% ethanol, stored at − 20°C, and deposited as vouchers in the Biodiversity Museum, Henan University, Kaifeng, China (HENU). Species identification was initially based on external morphology and subsequently confirmed by genitalia dissection following standard procedures [3]. Total genomic DNA was extracted from three legs from one side using the DNeasy Blood & Tissue Kit (Qiagen, Hilden, Germany) following the manufacturer's protocol, with the remaining tissues retained as vouchers. DNA quality and concentration were assessed via 1% agarose gel electrophoresis and NanoDrop 2000 spectrophotometry (Thermo Fisher Scientific, Waltham, MA, USA). The lasiocampid specimens were sent to Beijing Berry Genomics Corporation for paired-end 150 bp high-throughput sequencing on the Illumina NovaSeq 6000 platform [24], which generated ≥ 12 GB of raw data.

Table 1
Sampling information of the 12 lasiocampid species sequenced in this study

Species	Locality	Altitude	Coordinates	Date
Arguda vinata	Tianchi Nature Reserve, Yunnan, China	2,103m	26.06°N, 99.28°E	2024.7.24
Baodera khasiana	Gaoligongshan Nature Reserve, Yunnan, China	2,468m	25.97°N, 98.71°E	2025.8.20
Cerberolebeda styx	Gaoligongshan Nature Reserve, Yunnan, China	2,141m	24.82°N, 98.77°E	2025.8.02
Crinocraspeda torrida	Wuliyan Mountain, Sichuan, China	1,300m	28.19°N, 105.06°E	2024.7.21
Eteinopla signata	Qingyun Temple, Fujian China	211m	25.78°N, 118.95°E	2025.6.10
Lebeda nobilis	Shiwandashan Nature Reserve, Guangxi, China	1,000m	21.71°N, 107.49°E	2023.8.25
Metanastria hyrtaca	Mopanshan Forest Park, Yunnan, China	2,276m	23.94°N, 101.96°E	2025.7.23
Micropacha zojka	Xishui Nature Reserve, Guizhou, China	881m	28.50°N, 106.40°E	2025.8.11
Pachypasoides clarilimbata	Zixishan Nature Reserve, Yunnan, China	2,309m	24.99°N, 101.40°E	2025.7.25
Pyrosis rotundipennis	Gaoligongshan Nature Reserve, Yunnan, China	2,141m	24.82°N, 98.76°E	2025.8.01
Radhica flavovittata	Pingheliang Nature Reserve, Shaanxi, China	1,526m	33.43°N, 108.44°E	2024.8.30
Takanea excisa	Tianchi Nature Reserve, Yunnan, China	2,103m	26.06°N, 99.28°E	2024.7.24

Mitochondrial genome assembly and annotation

Raw data were quality-filtered using BBTools v38.89 [25] to remove duplicates, trim low-quality bases from both ends, and correct erroneous base pairs. The complete mitochondrial genome was assembled using Novoplasty v4.3.1 [26], with the complete mitochondrial genome of *Dendrolimus punctatus* (GenBank accession: NC027156) as the seed reference. The assembled circular genome was imported into Geneious Prime v2026.0 [27] for annotation of protein-coding genes (PCGs) and ribosomal RNA genes (rRNAs) by alignment with the reference genome. Start and stop codons of PCGs were manually verified through ORF prediction and comparison with homologous sequences. Transfer RNA (tRNA) genes were predicted using MITOS2 [28], and their secondary structures were further confirmed manually. The non-coding control region was identified based on its location between *rrnS* and *trnI*. The

annotated mitochondrial genome sequences have been submitted to GenBank under the accession numbers PZ210156–PZ210160, PZ368139–PZ368144, and PZ369173.

Genome characterization and comparative analyses

Circular maps of the 12 sequenced mitochondrial genomes were generated using OGDraw [29]. Base composition, AT-skew, and GC-skew were calculated using PhyloSuite v2 [30]. Relative synonymous codon usage (RSCU) for the 13 PCGs was calculated and visualized using the R v4.5.2 script *RSCUPlot.R* [31]. Nucleotide diversity (Pi) was estimated using DnaSP6 [32] with a sliding window approach (window size: 200 bp, step size: 25 bp) to examine variation patterns across PCGs. The ratio of non-synonymous (Ka) to synonymous (Ks) substitution rates for PCGs was calculated using KaKs_Calculator 3.0 [33, 34] to assess evolutionary selection pressures. Genetic distances among species were computed based on the Kimura 2-parameter (K2P) model using MEGA v11 [35]. tRNA secondary structures were visualized using the Python script *TrnaStructureBeautifier.py* [31]. Comparative genomic analyses among the 12 mitogenomes were conducted using BLAST+ v2.17.0 [36], and sequence similarity was visualized using the BLAST Ring Image Generator (BRIG) [37].

Phylogenetic analyses

The 13 PCGs and two rRNAs were extracted from the mitochondrial genomes of 25 lasiocampid species using PhyloSuite v2, with four species of the genus *Bombyx* (*B. huttoni*, *B. lemeepauli*, *B. mori*, and *B. mandarina*) selected as outgroups. The PCGs and rRNA genes were aligned using MACSE v2.03 [38] and MAFFT v7.471 [39], respectively, with ambiguously aligned regions in PCG removed using Gblocks 0.91b [40] and gap positions in rRNAs trimmed using trimAl [41]. The aligned sequences were concatenated into a single dataset for subsequent analyses. The best-fit nucleotide substitution model for maximum likelihood (ML) analysis was selected using ModelFinder v2.2.0 [42], and the ML tree was reconstructed using IQ-TREE v2.2.0 [43] with 5,000 ultrafast bootstrap replicates. For Bayesian inference (BI), the optimal partitioning scheme and models were determined using PartitionFinder2 [44], and the BI tree was reconstructed using MrBayes v3.2.7a [45] with two independent runs of 2,000,000 generations, sampling every 100 generations, and discarding the first 25% of trees as burn-in. Phylogenetic trees were visualized and edited using the iTOL v6 [46] and Adobe Illustrator 2024 [47].

Results

Basic structure and nucleotide composition of mitochondrial genomes

The complete mitochondrial genomes of the 12 lasiocampid species were typical circular double-stranded molecules, ranging from 15,387 to 15,938 bp in length. Size variation among genomes was mainly attributable to length differences in the non-coding region. All 12 mitochondrial genomes

contained the standard set of 13 protein-coding genes (PCGs), 22 transfer RNA genes (tRNAs), and two ribosomal RNA genes (rRNAs), and one non-coding control region, with no gene loss (Fig. 1).

Nucleotide composition exhibited a pronounced AT bias, with AT contents exceeding 77.0% in all 12 mitogenomes. Among the sequenced species, *Pachypasoides clarilimbata* showed the lowest AT content (77.4%), while *Cerberolebeda styx* and *Takanea excisa* exhibited the highest (both 81.3%), with most genomes ranging from 79.0% to 81.0%. AT-skew values were positive (0.001–0.042) in all species except *T. excise* (− 0.002), whereas GC-skew values were consistently negative across all species, ranging from − 0.291 to − 0.200 (Fig. 2A; Additional file 1).

Protein-coding genes and codon usage

The total length of the 13 PCGs ranged from 11,178 to 11,232 bp across the 12 mitogenomes, with AT contents varying from 75.2 to 79.3% (exceeding 79.0% in *C. styx*, *M. zojka*, and *T. excisa*). AT-skew values were negative in all species, ranging from − 0.149 to − 0.122, whereas GC-skew values were positive (0.012–0.036) in all except *P. rotundipennis* (− 0.014) (Fig. 2B; Additional file 1).

Most PCGs utilized ATN (ATA/ATC/ATG/ATT) as start codon, with the following exceptions: *cox1* employed CGA in all species; *nad4L* used TTG in *A. vinata* and *P. rotundipennis*; and *nad1* used GTG in *L. nobilis*. For termination codons, *cox1* (except in *L. nobilis*), *cox2, nad4* (except in *E. signata* and *M. zojka*), and *nad5* (*E. signata* and *M. zojka*) used the incomplete termination codon T; all other PCGs used TAA or TAG (Additional file 2). The 12 mitogenomes exhibited similar relative synonymous codon usage (RSCU) patterns, with UUA (Leu1) being the most frequently used codon. Codons ending with A or U were significantly more prevalent than those ending with G or C, reflecting the strong AT bias observed in the PCGs (Fig. 3).

Transfer and ribosomal RNA genes

The 22 tRNA genes had a combined length ranging from 1,452 to 1,493 bp in total length across the 12 mitogenomes, with AT contents exceeding 80.0% in all species and reaching 82.3% in *C. styx* (Fig. 2C; Additional file 1). Secondary structure prediction revealed that 21 of the 22 tRNAs folded into the canonical cloverleaf configuration, whereas *trnS1* lacked the dihydrouridine (DHU) arm and formed a simple loop (Additional file 3). The two rRNA genes, *rrnL* and *rrnS*, were located between *trnL2* and *trnV*, and between *trnV* and the control region, respectively. The *rrnL* gene ranged from 1,364 to 1,473 bp, while the *rrnS* gene ranged from 776 to 783 bp, with both exhibiting AT contents exceeding 82.0% (Fig. 2D; Additional file 1).

Overlapping sequences and non-coding regions

A total of 16 gene overlaps were identified across the 12 mitogenomes, with three overlaps (*atp8-atp6*, *trnW-trnC*, and *nad2-trnW*) present in all genomes, and *trnI-trnQ* (TTA) found in ten genomes (Additional

file 4). The non-coding control region was located between *rrnS* and *trnM* in all species except *A. vinata*, where it was positioned between *rrnS* and *trnI*. This region exhibited marked length variation among species, ranging from 134 bp in *A. vinata* to 847 bp in *C. styx*. AT content of the control region exceeded 90.0% in all species except *B. khasiana* (89.7%) (Additional file 5).

Nucleotide diversity and evolutionary rates

Sliding window analysis of the 13 PCGs across the 12 mitogenomes revealed variable nucleotide diversity (Pi), with *nad6* showing relatively high values (> 0.18), while the remaining genes exhibited Pi values mainly between 0.12 and 0.16 (Fig. 4). Pairwise genetic distance analysis indicated that *atp8* and *nad6* exhibited relatively high K2P distances, whereas *cox1* and *nad1* showed relatively low genetic distances, suggesting that the former evolved faster while the latter were more conserved (Fig. 5A). The Ka/Ks ratios (ω) of all 13 PCGs were far less than 1, indicating strong purifying selection. Among them, *atp8* exhibited a relatively higher ω value, while *cox1* showed the lowest (Fig. 5B).

Comparative homology analysis and gene rearrangement

Multiple sequence alignment of the 12 mitogenomes revealed high sequence similarity, with pairwise identities exceeding 70.0% across almost all comparisons (Fig. 6). Comparative analysis of gene arrangements among the 12 mitogenomes identified only one distinct rearrangement: the gene order *trnI–trnM–trnQ* was observed in *A. vinata*, whereas the other 11 species shared the *trnM–trnI–trnQ* arrangement. This conserved gene order across the majority of species indicates a stable genomic architecture within Lasiocampidae (Fig. 7).

Phylogenetic analyses

Our phylogenetic analyses recovered Lasiocampidae as a well-supported monophyletic clade (BS = 100, PP = 1) (Fig. 8). Within the family, *Trabala* and *Crinocraspeda* formed a sister group (BS = 99, PP = 1) and together constituted the earliest diverging lineage. The remaining genera were progressively nested as follows: *Apatelopteryx* was recovered as sister to a clade comprising *Eteinopla* + *Euthrix* and *Micropacha*; this lineage then formed a sister relationship with *Gastropacha*. Subsequently, the clade of *Arguda* + *Takanea* grouped with *Radhica*, and together they formed a sister relationship with the *Baodera* + *Cerberolebeda* clade. *Dendrolimus* and *Pachypasoides* formed a sister pair, and this clade grouped with *Kunugia*; this clade together formed a clade with *Lebeda* (the sister group of *Metanastria* + *Pyrosis*) and *Streblote*.

Discussion

Mitochondrial genome characteristics

The 12 newly sequenced lasiocampid mitogenomes exhibited the typical circular structure of most Lepidoptera, ranging from 15,387to 15,938 bp, with size variation primarily reflecting length differences

in the non-coding control region [48]. Each genome contained the standard set of 37 genes, with gene order and orientation identical to other lepidopteran mitogenomes, including the *trnM–trnI–trnQ* arrangement considered a molecular synapomorphy for Lepidoptera [49–52], likely originating from tandem duplication and random loss (TDRL) events during early lepidopteran evolution [53]. Three gene overlaps (*atp8–atp6, trnW–trnC, and nad2–trnW*) were consistently present across all genomes, suggesting functional constraints on these regions [54].

The mitogenomes showed a pronounced AT bias (> 77.0%), typical of Lepidoptera, with PCGs exhibiting lower AT content than the control region, and this difference likely reflects stronger functional constraints on coding sequences [55]. AT-skew and GC-skew analyses revealed the typical metazoan pattern (positive AT-skew, negative GC-skew [56], except for *T. excisa* with a slight negative AT-skew, a phenomenon also documented in other lepidopteran groups [57]. This strand-specific asymmetry is commonly attributed to asymmetric mutational pressures during mtDNA replication and transcription, particularly the differential susceptibility of strands to deamination [58].

TrnS1 lacked DHU arms in all 12 genomes, a conserved feature in lepidopteran mitogenomes that does not impair tRNA function [59]. Most PCGs used ATN as start codons, with rare codons (GTG, TTG) observed in some genes that are typically edited to ATN during transcription [60, 61]. The *cox1* gene employed CGA as start codon in all species, a common feature in Lepidoptera [13]. Incomplete stop codons (single T) frequently occurred in *cox1*, *cox2*, *nad4*, and *nad5*, and are typically completed via post-transcriptional polyadenylation to form TAA [62–66]. RSCU analysis revealed a significant preference for A/T-ending codons, consistent with the AT-rich nature of these mitogenomes and suggesting that compositional forces, rather than adaptive optimization, predominantly drive mitochondrial codon usage evolution [67].

Nucleotide diversity and evolutionary rates of PCGs

The sliding window and pairwise genetic distance analyses revealed notable evolutionary heterogeneity among the 13 PCGs. *nad6* exhibited the highest nucleotide diversity, while *atp8* and *nad6* showed the largest genetic distances, indicating faster evolutionary rates for these two genes. In contrast, *cox1* displayed lower genetic distances and appeared relatively conserved, consistent with previous findings in Lepidoptera [68].

The Ka/Ks ratios of all 13 PCGs were considerably less than 1, indicating strong purifying selection that removes deleterious mutations to preserve essential mitochondrial functions [69, 70]. Among the PCGs, *atp8* exhibited the highest Ka/Ks ratio and *cox1* the lowest, suggesting that genes with distinct functional roles in oxidative phosphorylation are subject to differential selective constraints. The relatively relaxed selection on *atp8* and *nad6*, together with the conserved nature of *cox1*, is consistent with patterns observed in other insect mitochondrial genomes [71]. These contrasting evolutionary rates among mitochondrial genes may have implications for marker selection in phylogenetic and population genetic studies of Lasiocampidae.

Phylogenetic relationships

Our ML and BI analyses based on 13 PCGs and two rRNAs recovered Lasiocampidae as a well-supported monophyletic clade, with most internal nodes receiving strong support (Fig. 8). This robust phylogenetic framework allowed us to clarify several long-standing uncertainties regarding generic relationships within the family. *Trabala* and *Crinocraspeda* were recovered as sister taxa, together forming the earliest diverging lineage within Lasiocampidae. This result resolves the previously ambiguous phylogenetic position of *Crinocraspeda* and supports the early-diverging status of *Trabala* [19]. Previous studies have largely relied on single-gene (e.g., *cox1*) or limited taxa sampling, which may have obscured deeper divergence events within the family. The inclusion of *Pachypasoides* in our analyses, which was absent in earlier studies, revealed a novel topology in which *Dendrolimus* and *Pachypasoides* formed a well-supported clade with *Kunugia*. This finding highlights the importance of comprehensive taxonomic sampling for resolving phylogenetic relationships in Lasiocampidae.

Our analyses also recovered several highly supported sister-group relationships that corroborate morphological evidence. *Arguda* and *Takanea* share broad, short forewings with obtuse-rounded apices and undulate outer margins, as well as similarities in male genital structures. *Baodera* and *Cerberolebeda* are both oligotypic genera with restricted geographical distributions. *Metanastria* and *Pyrosis* exhibit commonalities in larval chaetotaxy [3]. *Eteinopla* and *Euthrix* also formed a strongly supported clade. These results provide robust molecular support for morphologically based groupings that had previously lacked rigorous phylogenetic validation. The congruence between molecular phylogeny and morphological characters in these clades reinforces the utility of integrative approaches for taxonomic revisions in Lasiocampidae.

Conclusions

In this study, we sequenced and assembled the mitogenomes of 12 lasiocampid species, 11 of which are reported here for the first time. The mitogenomes exhibit conserved gene arrangement and strong AT bias, with only one rearrangement detected. Evolutionary rates vary among PCGs: atp8 and nad6 evolve fastest, while cox1 is most conserved. This pattern may inform marker selection for future studies. Phylogenetic analyses recovered Lasiocampidae as monophyletic and resolved several key generic relationships. These genomic and phylogenetic data provide a solid foundation for taxonomic revisions, evolutionary biology, and biogeography of Lasiocampidae.

Declarations

Acknowledgements

We thank Haoran Wang, Hang Zhou, Weiqi Liao, and Yating Zhu for their assistance with specimen collection. Special thanks to Haipeng Zhao for his constructive comments on the manuscript.

Authors' contributions

KG designed the project, YLP, YKL performed genome assembly, annotation and data analyses, KG, YLP wrote the manuscript. KG, JY revised the manuscript. All authors read and approved the final manuscript.

Funding

This research was supported by the National Natural Science Foundation of China (Grant number 32300379), the Key Research Project of Colleges and Universities in Henan Province (Grant number 26A180005), and Xinyang Academy of Ecological Research Open Foundation (Grant No. 2023XYMS03).

Data availability

The genome sequence data supporting the findings of this study were publicly available in GenBank (NCBI) under accession numbers PZ210156–PZ210160, PZ368139–PZ368144, and PZ369173.

Ethics approval and consent to participate

Not applicable.

Consent for publication

Not applicable.

Competing interests

The authors declare no competing interests.

Author details

[1] School of Life Sciences, Henan University, Kaifeng 475004, Henan, China

[2] Henan Dabieshan National Field Observation and Research Station of Forest Ecosystem, Kaifeng 475004, Henan, China

References

1. Beccaloni G, Scoble M, Kitching I, Simonsen T, Robinson G, Pitkin B et al. *Global Lepidoptera Index* (D. Hobern, Ed.; 1.1.26.129). 2026.
2. Pu YL, Yan TZ, Wang HR, Gao K, Zhao HP. The first chromosome-level genome of the lappet moth *Trabala vishnou* (Lepidoptera: Lasiocampidae). Sci Data. 2025;12(1):1154.
3. Liu YQ, Wu CS. Fauna Sinica. Insecta. Volume 47: Lepidoptera. Lasiocampidae. Beijing, China: Science; 2006.
4. Liu YH. Damage of *Trabala vishnou gigantina* (Lepidoptera: Lasiocampidae) to the sea-buckthorn forest and its biological characteristic. Plant Prot. 2013;39:147–51.

5. Yang J, Xu JX, Zhao HP, Gao K. Comparative morphology of the larval mouthparts among six species of Lasiocampidae (Insecta, Lepidoptera). Zool Anz. 2026.
6. Yang J, Zhao HP, Gao K. Morphology and distribution of antennal sensilla in the lappet moth *Gastropacha quercifolia* (Lepidoptera: Lasiocampidae). J Morphol. 2026;287(6):e70145.
7. Li J. Dynamic changes of mitochondrial morphology and its biological significance. Biol Teach Middle Sch. 2014;6:43–5.
8. Zhang F, Mi ZY. Progress in molecular biology research of animal mitochondrial DNA. Prog Biotechnol. 1998;18(3):25–31.
9. Simon C, Frati F, Beckenbach A. Evolution, weighting, and phylogenetic utility of mitochondrial gene sequences and a compilation of conserved polymerase chain reaction primers. Ann Entomol Soc Am. 1994;87(6):651–701.
10. Cheng XY, Zhou HZ, Zhang GX. Perspective of molecular biological techniques applied in insect systematics. Zool Syst. 2000;25(2):121–33.
11. Cameron SL. Insect mitochondrial genomics: Implications for evolution and phylogeny. Annu Rev Entomol. 2014;59:95–117.
12. Boore JL. Animal mitochondrial genomes. Nucleic Acids Res. 1999;27(8):1767–80.
13. Qin J, Zhang YZ, Zhou X, Kong XB, Wei SJ, Ward RD, et al. Mitochondrial phylogenomics and genetic relationships of closely related pine moth (Lasiocampidae: *Dendrolimus*) species in China, using whole mitochondrial genomes. BMC Genomics. 2015;16(1):428.
14. Shtolz N, Mishmar D. The mitochondrial Genome–on selective constraints and signatures at the organism, cell, and single mitochondrion levels. Front Ecol Evol. 2019;7:342.
15. Huang XF, Sang JY, Yan LP, Zhang D. The phylogeny and evolution of blow flies (Diptera: Calliphoridae) from the perspective of mitogenomics. BMC Genomics. 2026;27(1):180.
16. Timmermans MJTN, Lees DC, Simonsen TJ. Towards a mitogenomic phylogeny of Lepidoptera. Mol Phylogenet Evol. 2014;79:169–78.
17. Regier JC, Cook CP, Mitter C, Hussey. A. A phylogenetic study of the 'bombycoid complex'(Lepidoptera) using five protein-coding nuclear genes, with comments on the problem of macrolepidopteran phylogeny. Syst Entomol. 2008;33(1):175–89.
18. Mutanen M, Wahlberg N, Kaila L. Comprehensive gene and taxon coverage elucidates radiation patterns in moths and butterflies. Proc R Soc B. 2010;277(1695):2839–48.
19. Wu LY, Xiong X, Wang XM, Xin TR, Wang J, Zou ZW, et al. The complete mitochondrial genome of *Trabala vishnou guttata* (Lepidoptera: Lasiocampidae) and the related phylogenetic analyses. Genetica. 2016;144(6):675–88.
20. Li D, Guo YR, Shao HJ, Tellier LC, Wang J, Xiang ZH, et al. Genetic diversity, molecular phylogeny and selection evidence of the silkworm mitochondria implicated by complete resequencing of 41 genomes. BMC Evol Biol. 2010;10(1):81.

21. Hu XL, Cao GL, Xue RY, Zheng XJ, Zhang X, Duan HR, et al. The complete mitogenome and phylogenetic analysis of *Bombyx mandarina* strain Qingzhou. Mol Biol Rep. 2010;37(6):2599–608.
22. Arunkumar KP, Metta M, Nagaraju J. Molecular phylogeny of silkmoths reveals the origin of domesticated silkmoth, *Bombyx mori* from Chinese *Bombyx mandarina* and paternal inheritance of *Antheraea proylei* mitochondrial DNA. Mol Phylogenet Evol. 2006;40(2):419–27.
23. Men QL, Xue GX, Mu D, Hu QL, Huang MY. Mitochondrial DNA markers reveal high genetic diversity and strong genetic differentiation in populations of *Dendrolimus kikuchii* Matsumura (Lepidoptera: Lasiocampidae). PLoS ONE. 2017;12(6):e0179706.
24. Modi A, Vai S, Caramelli D, Lari M. The illumina sequencing protocol and the NovaSeq 6000 system. Methods Mol Biol. 2021;2242:15–42.
25. Bushnell B, BBMap. June. Available online: https://sourceforge.net/projects/bbmap/ (accessed on 4 2026) 2014.
26. Dierckxsens N, Mardulyn P, Smits G. NOVOPlasty: de Novo assembly of organelle genomes from whole genome data. Nucleic Acids Res. 2017;45(4):e18.
27. Kearse M, Moir R, Wilson A, Stones-Havas S, Cheung M, Sturrock S, et al. Geneious basic: an integrated and extendable desktop software platform for the organization and analysis of sequence data. Bioinformatics. 2012;28(12):1647–9.
28. Bernt M, Donath A, Jühling F, Externbrink F, Florentz C, Fritzsch G, et al. MITOS: improved de Novo metazoan mitochondrial genome annotation. Mol Phylogenet Evol. 2013;69(2):313–9.
29. Lohse M, Drechsel O, Kahlau S, Bock R. OrganellarGenomeDRAW—a suite of tools for generating physical maps of plastid and mitochondrial genomes and visualizing expression data sets. Nucleic Acids Res. 2013;41(W1):W575–81.
30. Zhang D, Ye T, Gao FL, Jakovlić I, Zhang J, La Q, et al. PhyloSuite v2: The Development of an All-in-One, Efficient and Visualization-Oriented Suite for Molecular Dating Analysis and Other Advanced Features. Imeta. 2025;4(6):e70095.
31. Xue H. Genome structure and comparative genomic analysis of *Alectoris magna*. Yantai: Yantai University; 2024.
32. Rozas J, Ferrer-Mata A, Sanchez-DelBarrio JC, Guirao-Rico S, Librado P, RamosOnsins SE, et al. DnaSP 6: DNA sequence polymorphism analysis of large data sets. Mol Biol Evol. 2017;34:3299–02.
33. Zhang Z. KaKs_Calculator 3.0: calculating selective pressure on coding and non-coding sequences. Genomics Proteom Bioinform. 2022;20(3):536–40.
34. Hurst LD. The Ka/Ks ratio: diagnosing the form of sequence evolution. Trends Genet. 2002;18:486–7.
35. Tamura K, Stecher G, Kumar S. MEGA11: molecular evolutionary genetics analysis version 11. Mol Biol Evol. 2021;38(7):3022–7.
36. Camacho C, Coulouris G, Avagyan V, Ma N, Papadopoulos J, Bealer K, et al. BLAST+: architecture and applications. BMC Bioinformatics. 2009;10:1–9.

37. Alikhan NF, Petty NK, Ben Zakour NL, Beatson SA. BLAST ring image generator (BRIG): simple prokaryote genome comparisons. BMC Genomics. 2011;12:1–10.
38. Ranwez V, Douzery EJP, Cambon C, Chantret N, Delsuc F. MACSE v2: toolkit for the alignment of coding sequences accounting for frameshifts and stop codons. Mol Biol Evol. 2018;35(10):2582–4.
39. Katoh K, Standley DM. MAFFT multiple sequence alignment software version 7: improvements in performance and usability. Mol Biol Evol. 2013;30(4):772–80.
40. Talavera G, Castresana J. Improvement of phylogenies after removing divergent and ambiguously aligned blocks from protein sequence alignments. Syst Biol. 2007;56(4):564–77.
41. Capella-Gutiérrez S, Silla-Martínez JM, Gabaldón T. trimAl: a tool for automated alignment trimming in large-scale phylogenetic analyses. Bioinformatics. 2009;25(15):1972–3.
42. Kalyaanamoorthy S, Minh BQ, Wong TK, Von Haeseler A, Jermiin LS. ModelFinder: fast model selection for accurate phylogenetic estimates. Nat Methods. 2017;14(6):587–9.
43. Minh BQ, Schmidt HA, Chernomor O, Schrempf D, Woodhams MD, Von Haeseler A, et al. IQ-TREE 2: new models and efficient methods for phylogenetic inference in the genomic era. Mol Biol Evol. 2020;37(5):1530–4.
44. Lanfear R, Frandsen PB, Wright AM, Senfeld T, Calcott B. PartitionFinder 2: new methods for selecting partitioned models of evolution for molecular and morphological phylogenetic analyses. Mol Biol Evol. 2017;34(3):772–3.
45. Ronquist F, Teslenko M, Van Der Mark P, Ayres DL, Darling A, Höhna S, et al. MrBayes 3.2: efficient bayesian phylogenetic inference and model choice across a large model space. Syst Biol. 2012;61(3):539–42.
46. Letunic I, Bork P. Interactive Tree of Life (iTOL) v6: recent updates to the phylogenetic tree display and annotation tool. Nucleic Acids Res. 2024;52(W1):W78–82.
47. Hoppe J. Adobe Illustrator. 2nd ed. Santa Barbara, CA: Rocky Nook, Inc; 2020.
48. Cameron S, Beckenbach A, Dowton M. Evidence from mitochondrial genomics on interordinal relationships in insects. Arthropod Syst Phylogeny. 2006;64:27–34.
49. Chen M, Tian LL, Shi QH. Complete mitogenome of the lesser purple emperor *Apatura ilia* (Lepidoptera: Nymphalidae: Apaturinae) and comparison with other nymphalid butterflies. Zool Res. 2012;33(2):191–201.
50. Xuan SB, Song F, Cao LM. The complete mitochondrial genome of the butterfly *Euripus nyctelius* (Lepidoptera: Nymphalidae). Mitochondrial DNA A. 2016;27(4):2563–5.
51. Li Y, Shu JP, Hua KD, Zhang YB, Ying Y, Zhang W. Sequencing and analysis of the complete mitochondrial genome of *Garella ruficirra*. J Zhejiang A&F Univ. 2024;41(4):724–34.
52. Li J, Lv Q, Zhang XM, Han HL, Zhang AB. Characterization and phylogenetic analysis of the complete mitochondrial genome of *Laelia suffusa* (Lepidoptera: Erebidae, Lymantriinae). J Insect Sci. 2021;21(1):5.

53. Cameron SL. Insect mitochondrial genomics: Implications for evolution and phylogeny. Annu Rev Entomol. 2014;59:95–117.
54. Li H, Shao RF, Song N, Song F, Jiang P, Li ZH, et al. Higher-level phylogeny of paraneopteran insects inferred from mitochondrial genome sequences. Sci Rep. 2015;5(1):8527.
55. Li MY, Zhang D, Zhang JP, Liu DK, Yi XF, Li R. The first complete mitochondrial genome of common hedge blue *Acytolepis puspa* (Lepidoptera: Lycaenidae), and comparative genomic analysis within polyommatinae. Ecol Evol. 2026;16(4):e73326.
56. Liu S, Hou R, Zhang QF, Duan MN, Tang SB, Wang WS, et al. Comparative mitogenomic and phylogenetic insights from four newly sequenced tick mitochondrial genomes. Front Vet Sci. 2026;12:1678349.
57. Bian DD, Ye WT, Dai ML, Lu ZT, Li MX, Fang YL, et al. Phylogenetic relationships of Limacodidae and insights into the higher phylogeny of Lepidoptera. Int J Biol Macromol. 2020;159:356–63.
58. Haag-Liautard C, Coffey N, Houle D, Lynch M, Charlesworth B, Keightley PD. Direct estimation of the mitochondrial DNA mutation rate in *Drosophila melanogaster*. PLoS Biol. 2008;6(8):e204.
59. Yang FQ, Xiao J, Zhang XY, Shang YJ, Guo YD. First report and phylogenetic analysis of mitochondrial genomes of *Chrysomya villeneuvi* and *Sarcophaga genuforceps*. Insects. 2025;16(1):26.
60. Behura SK, Lobo NF, Haas B, deBruyn B, Lovin DD, Shumway MF, et al. Complete sequences of mitochondria genomes of Aedes aegypti and *Culex quinquefasciatus* and comparative analysis of mitochondrial DNA fragments inserted in the nuclear genomes. Insect Biochem Mol Biol. 2011;41(10):770–7.
61. Weigl S, Testini G, Parisi A, Dantas-Torres F, Traversa D, Colwell DD, et al. The mitochondrial genome of the common cattle grub, *Hypoderma lineatum*. Med Vet Entomol. 2010;24(3):329–35.
62. Wang XC, Sun XY, Sun QQ, Zhang DX, Hu J, Yang Q, et al. Complete mitochondrial genome of the laced fritillary *Argyreus hyperbius* (Lepidoptera: Nymphalidae). Zool Res. 2011;32(5):465–75.
63. Tian LL, Chen M, Sun XY, Gai YH, Hao JS, Yang Q. Complete mitochondrial genome of the five-dot sergeant *Parathyma sulpitia* (Nymphalidae: Limenitidinae) and its phylogenetic implications. Zool Res. 2012;33(2):133–43.
64. Chen L, Wahlberg N, Liao CQ, Wang CB, Ma FZ, Huang GH. Fourteen complete mitochondrial genomes of butterflies from the genus *Lethe* (Lepidoptera, Nymphalidae, Satyrinae) with mitogenome-based phylogenetic analysis. Genomics. 2020;112(6):4435–41.
65. Schuster G, Stern D. RNA polyadenylation and decay in mitochondria and chloroplasts. Prog Mol Biol Transl Sci. 2009;85:393–422.
66. Ojala D, Montoya J, Attardi G. tRNA punctuation model of RNA processing in human mitochondria. Nature. 1981;290(5806):470–74.
67. Medina NS, Moreno-Carmona M, Canal NA, Prada-Quiroga CF. Mitochondrial genome variations and possible adaptive implications in some Tephritid flies (Diptera, Tephritidae). Int J Mol Sci. 2025;26(12):5560.

68. Jiang F, Yu XD, Sun ET, Gu SL, Liu Y, Liu T. Mitochondrial genomes of four slug moths (Lepidoptera, Limacodidae): Genome description and phylogenetic implications. Ecol Evol. 2024;14(5):e11319.
69. Broughton RE, Reneau PC. Spatial covariation of mutation and nonsynonymous substitution rates in vertebrate mitochondrial genomes. Mol Biol Evol. 2006;23(8):1516–24.
70. Hu YJ, Jia FF, Hu L, Wu C, Tian T, Li TJ, et al. Comparative mitogenome research revealed the phylogenetics and evolution of the superfamily Tenebrionoidea (Coleoptera: Polyphage). Ecol Evol. 2024;14(6):e11520.
71. Liu N, Fang LJ, Zhang YL. The complete mitochondrial genomes of four species in the subfamily Limenitidinae (Lepidoptera, Nymphalidae) and a phylogenetic analysis. Insects. 2021;13(1):16.

Figures

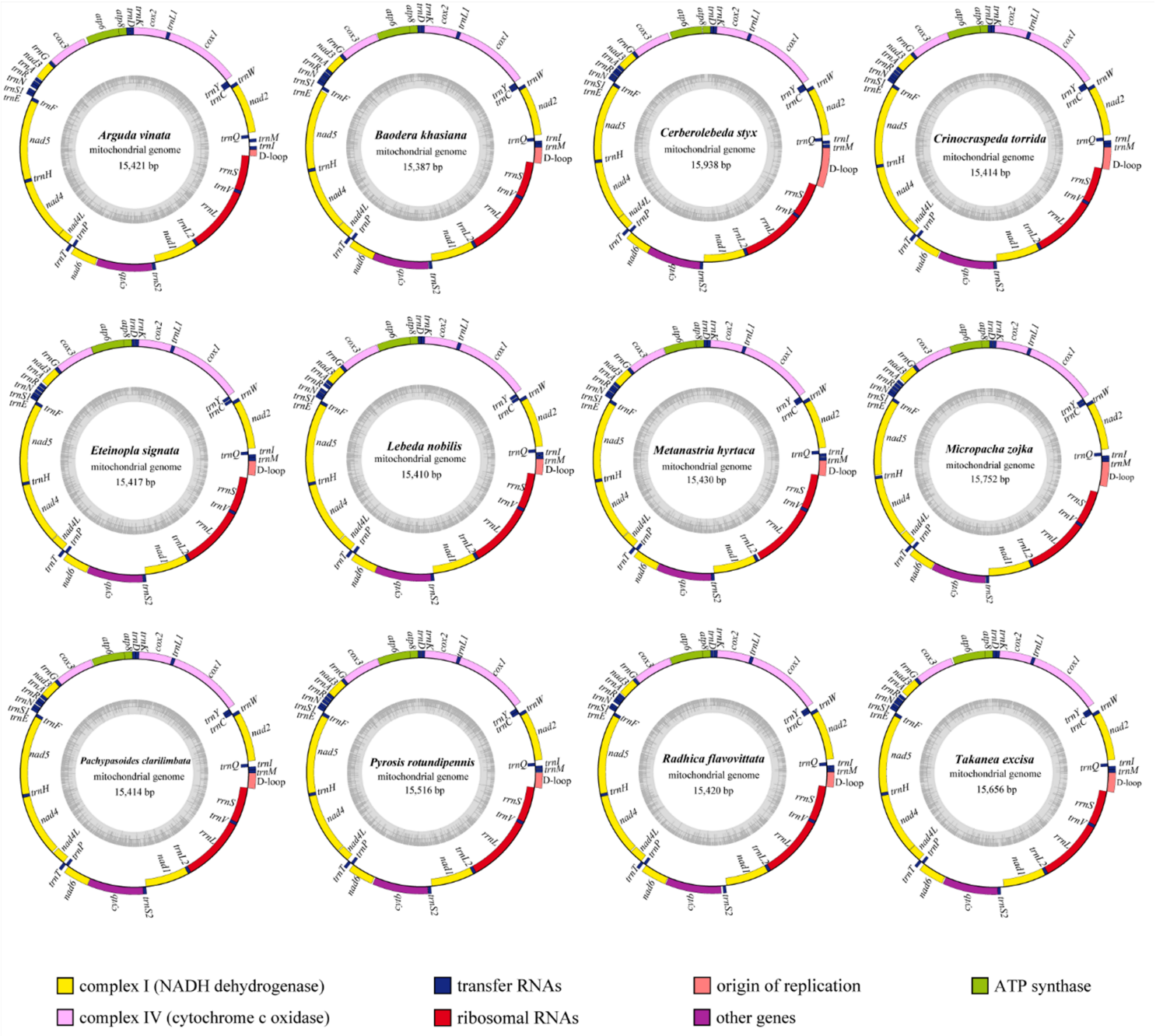


Figure 1

Circular maps of the mitochondrial genomes of twelve Lasiocampidae species. Genes outside and inside the outer circle are transcribed clockwise and counterclockwise, respectively. Colors denote functional gene groups; dark gray in the inner circle indicates GC content.

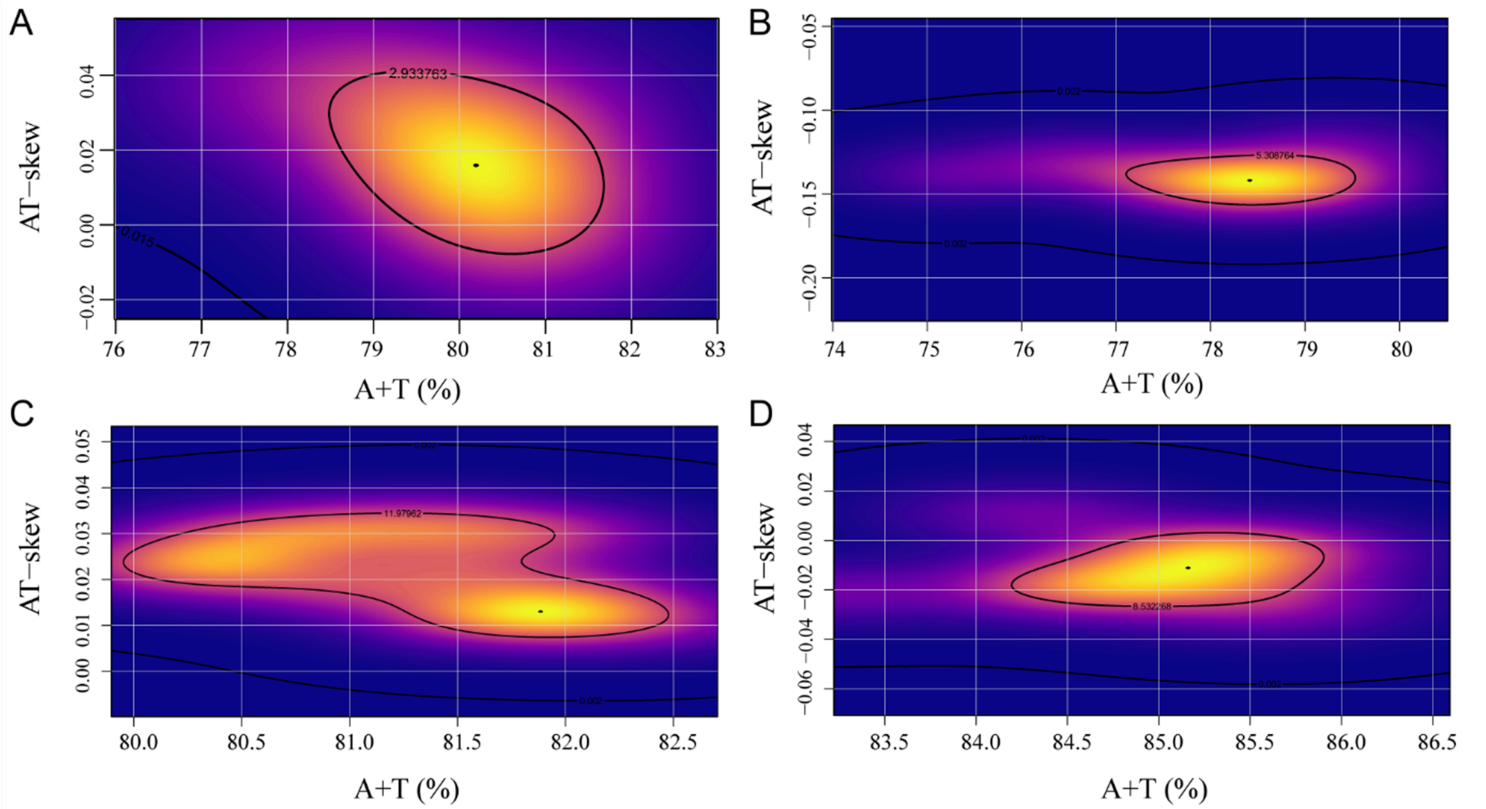


Figure 2

AT-skew vs. A+T content for the 12 lasiocampid mitogenomes. **A** Whole genome, **B** PCGs, **C** tRNAs, and **D** rRNAs.

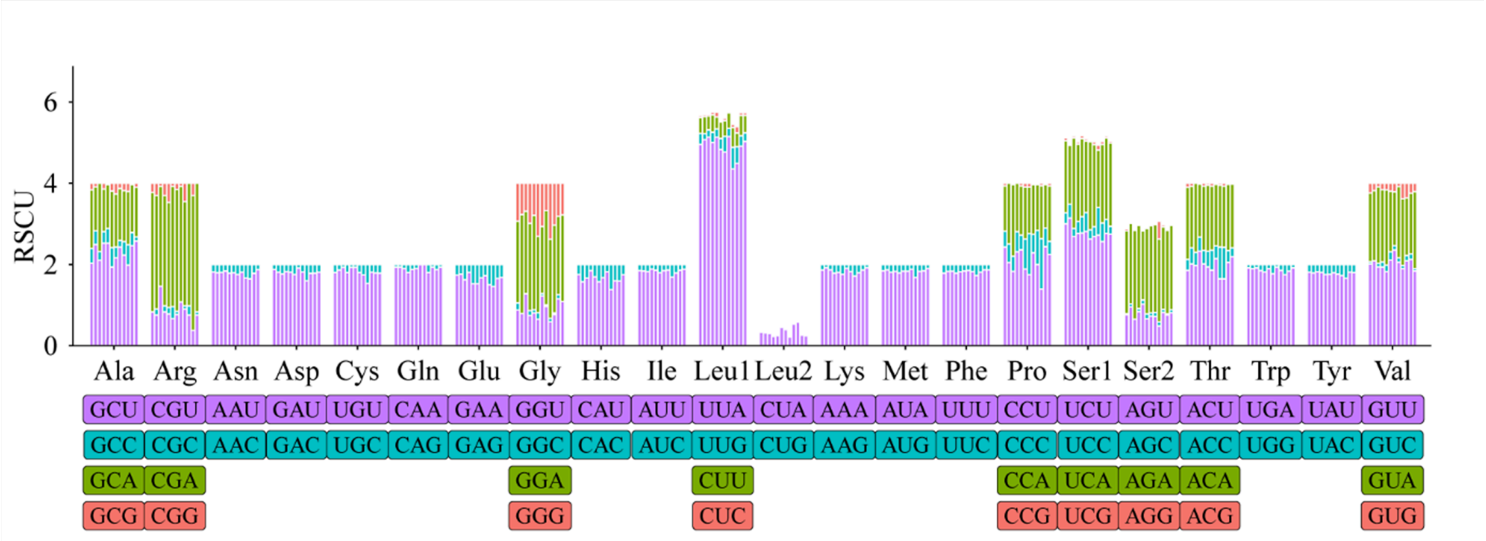


Figure 3

Relative synonymous codon usage (RSCU) of the 13 protein-coding genes in the 12 lasiocampid mitogenomes.

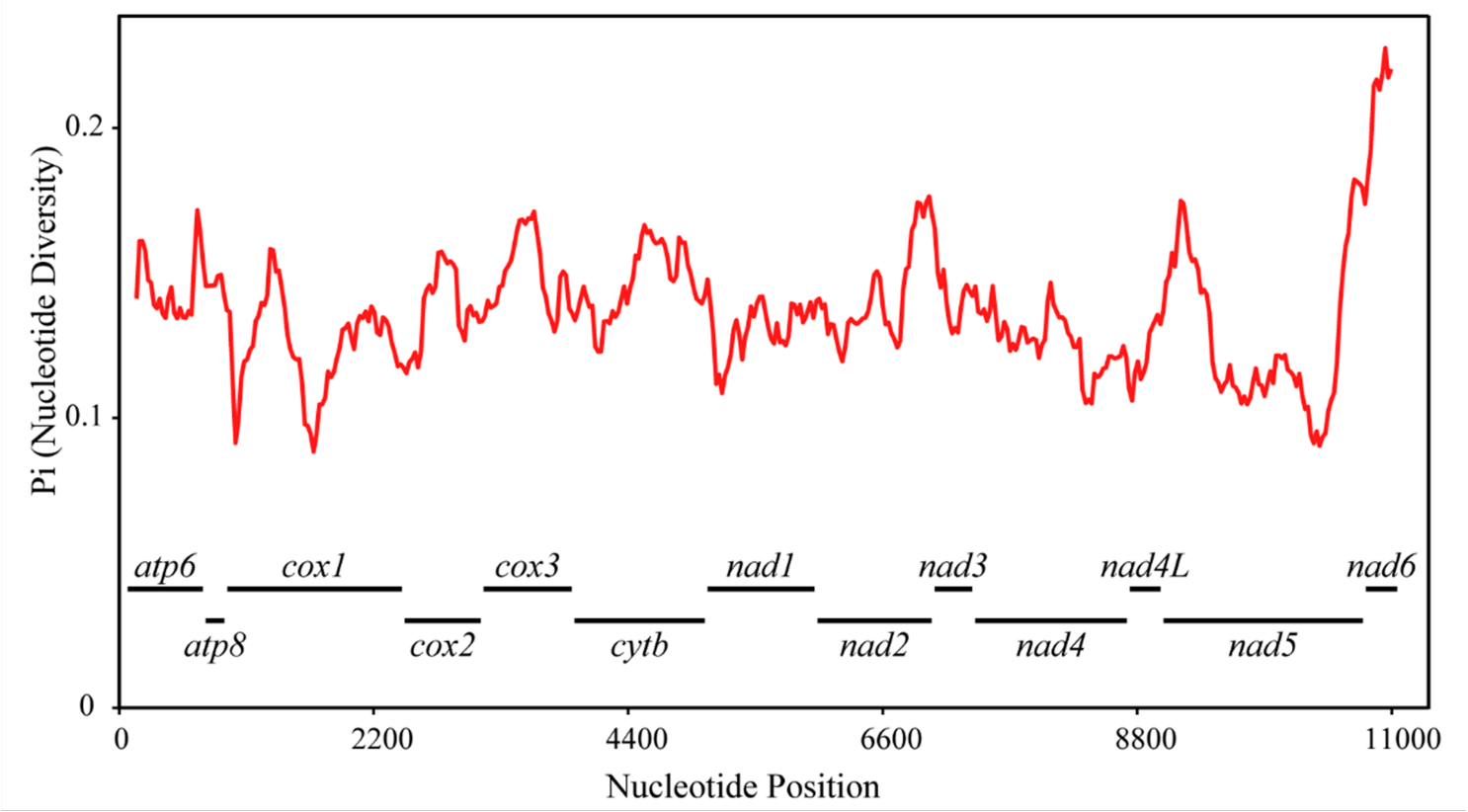


Figure 4

Sliding window analysis of 13 protein-coding genes of 12 lasiocampid mitogenomes. The red curve shows the values of nucleotide diversity (Pi).

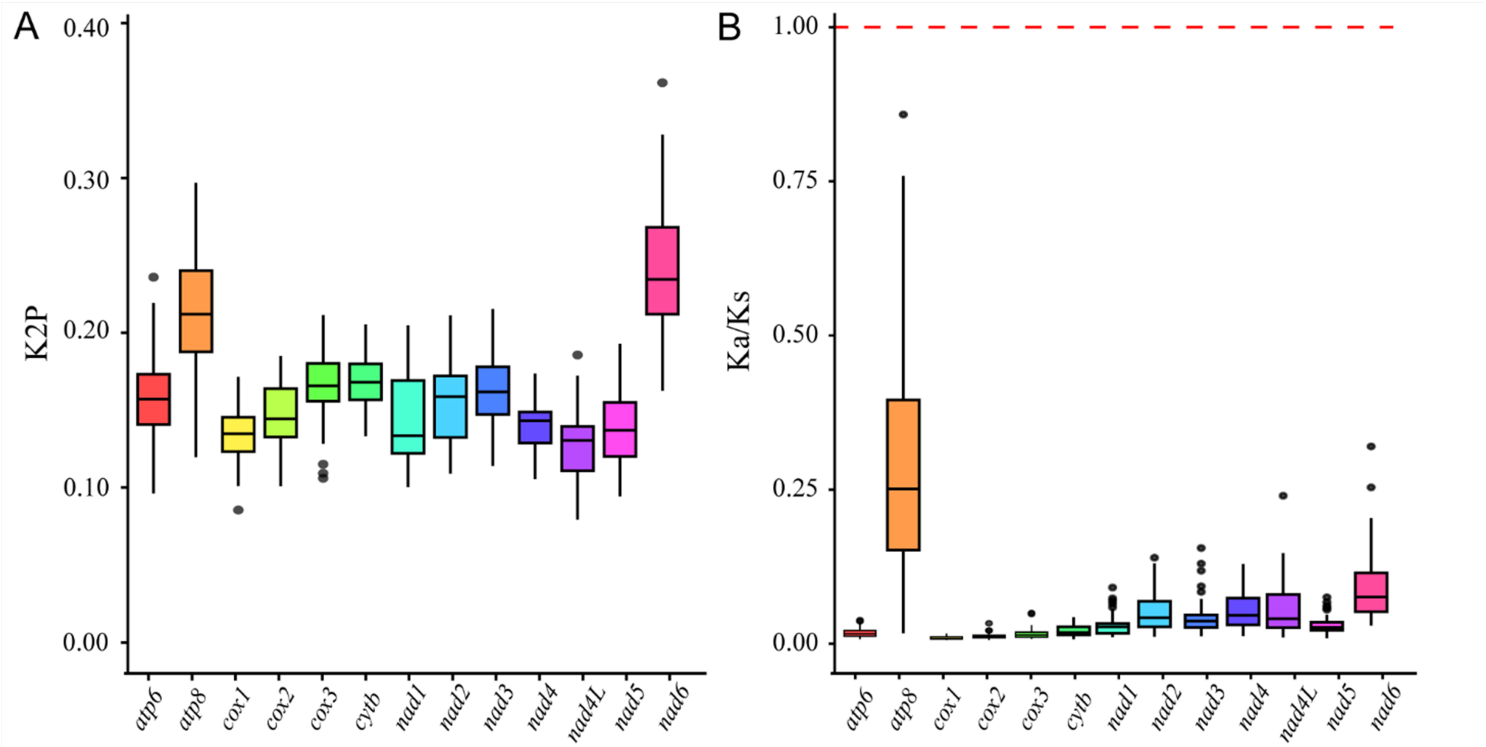


Figure 5

A Genetic distance (Kimura 2-parameter model) for each protein-coding gene among the 12 lasiocampid species; **B** Ka/Ks ratios (ω) for each protein-coding gene. Values below 1 indicate purifying selection.

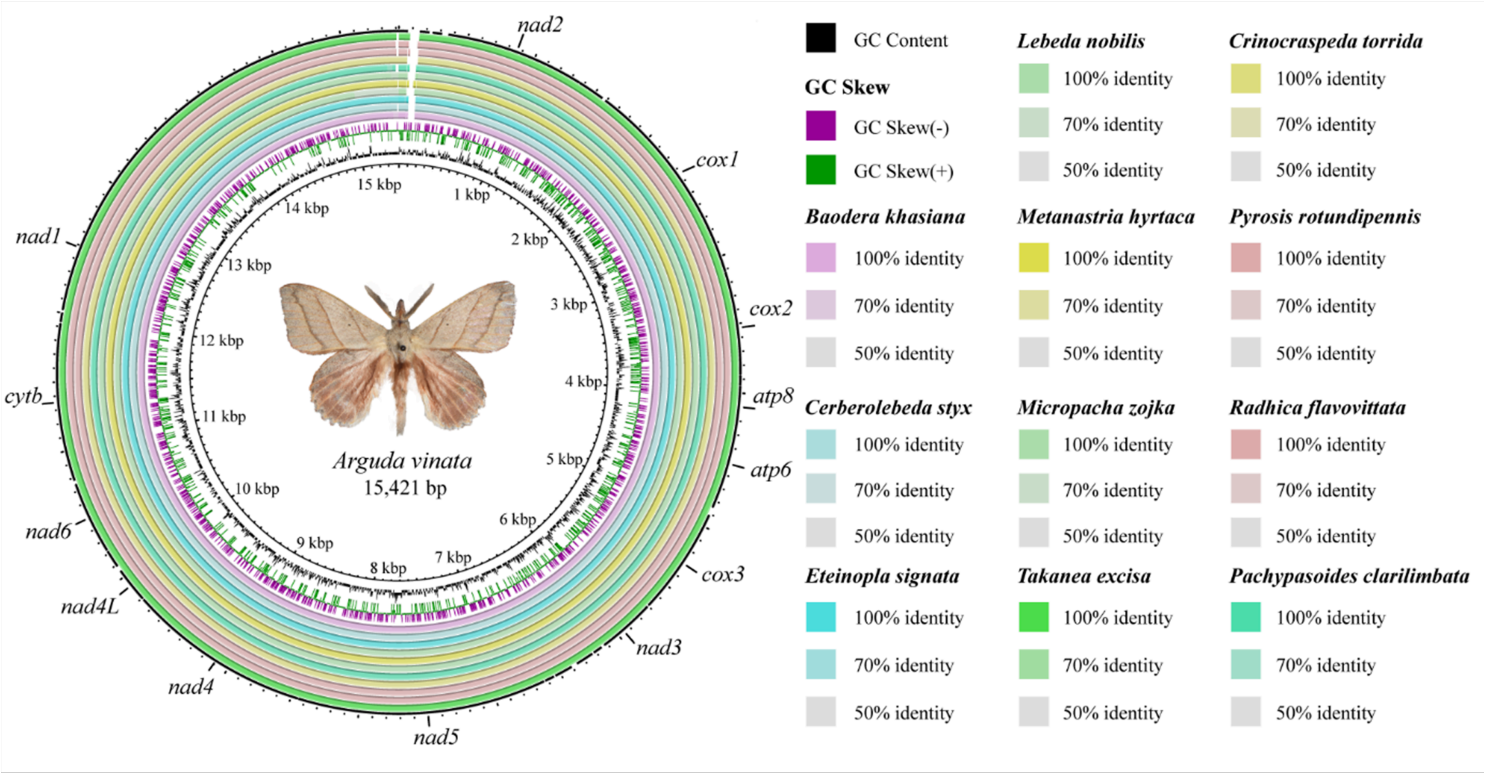


Figure 6

Comparative genomic analysis of the 12 lasiocampid mitogenomes using BLAST with *Arguda vinata* as the reference. The outermost circle shows protein-coding genes (black). Each subsequent circle represents one species, with colors indicating sequence similarity to the reference genome.

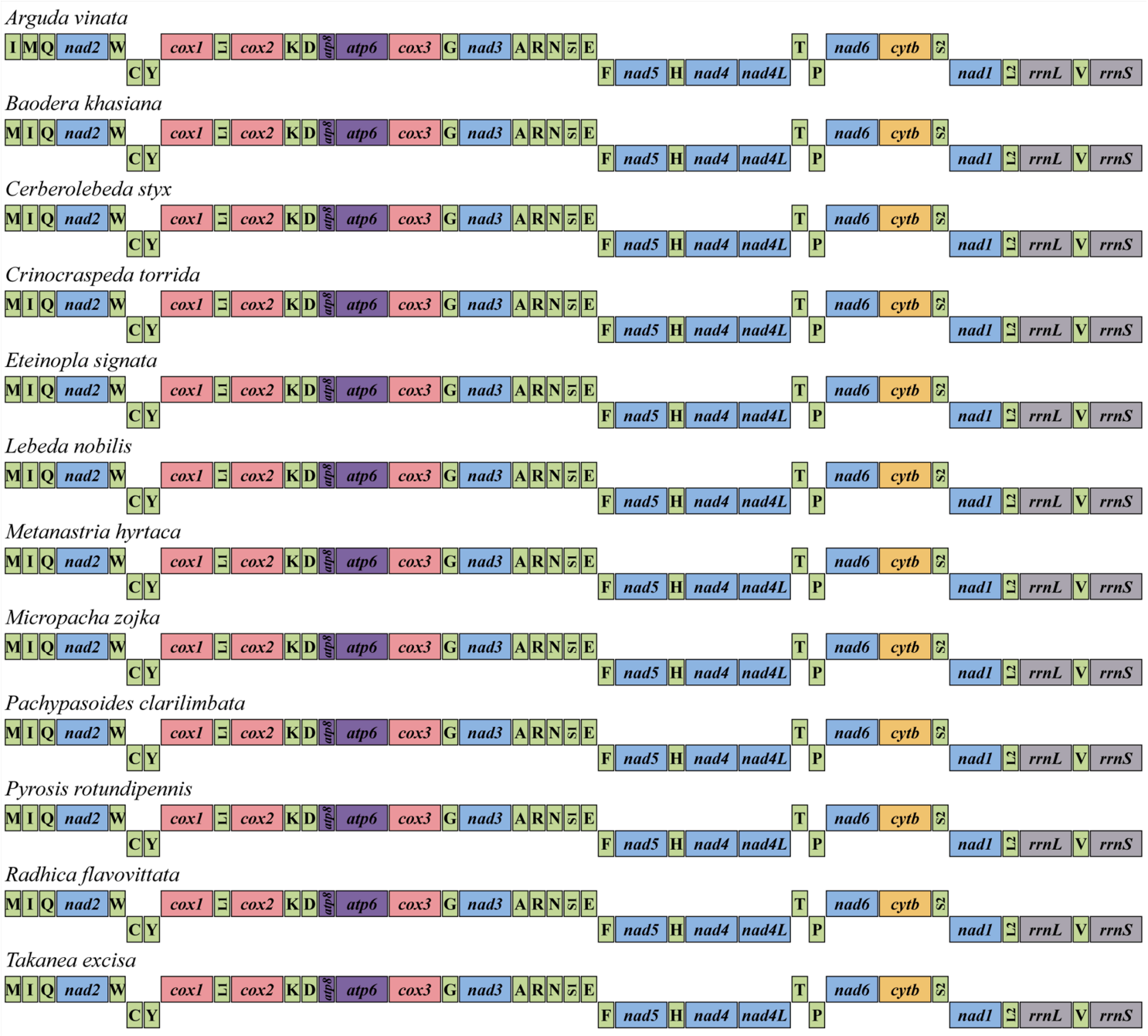


Figure 7

Comparison of mitochondrial gene arrangements among the 12 lasiocampid species. Colored blocks represent different genes, with arrows indicating transcription direction. All species share a conserved gene order, except *Arguda vinata*, which shows a rearrangement of the *trnI–trnM–trnQ* region.

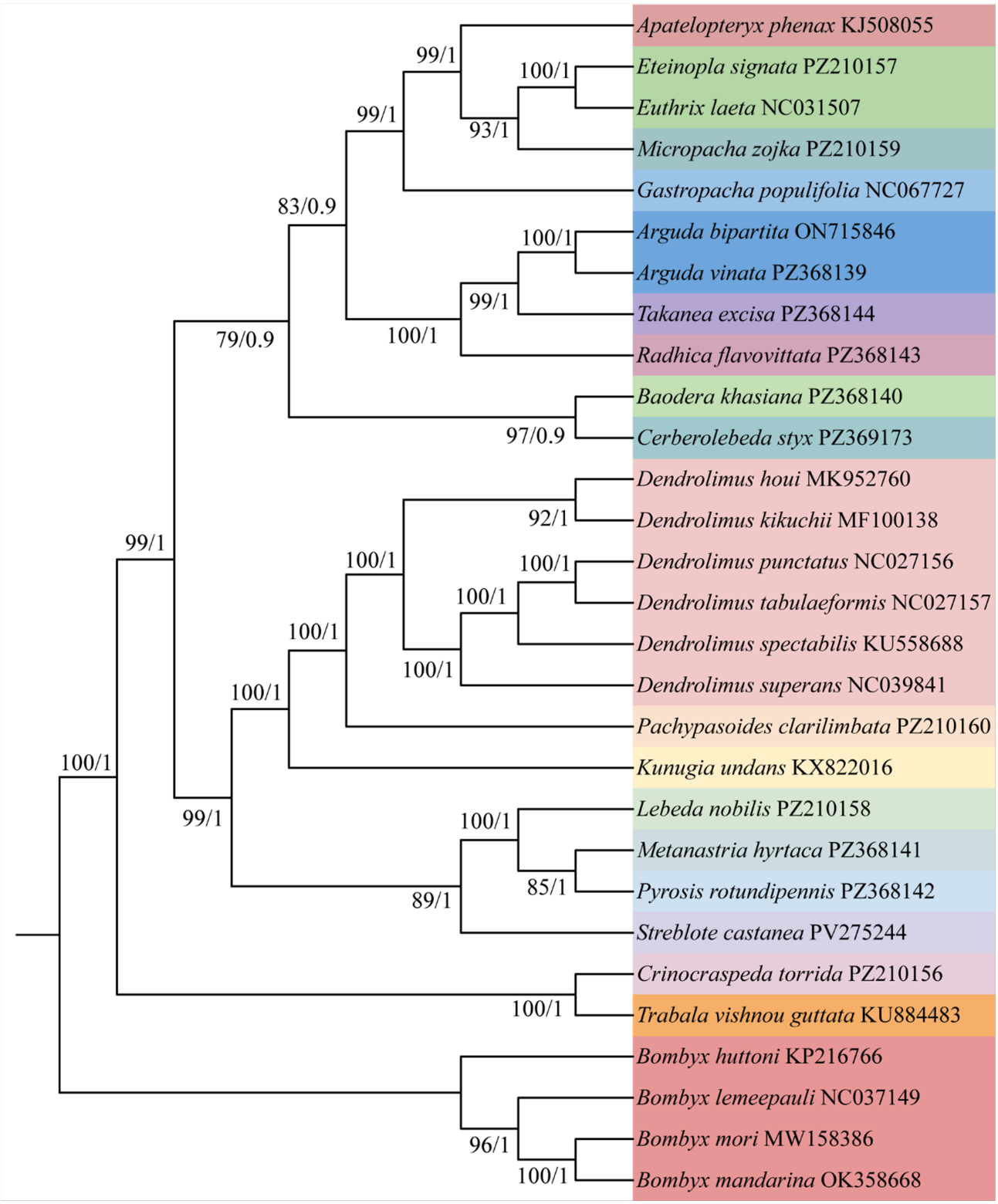


Figure 8

Phylogenetic tree of Lasiocampidae reconstructed from 13 PCGs and two rRNAs. Numerals at nodes indicate ML bootstrap values (BS) and Bayesian posterior probabilities (PP), respectively (BS/PP). Different colors represent distinct generic clades.

Supplementary Files

This is a list of supplementary files associated with this preprint. Click to download.

- SupplementaryMaterial1.docx
- SupplementaryMaterial2.docx
- SupplementaryMaterial3.docx
- SupplementaryMaterial4.docx
- SupplementaryMaterial5.docx